energy&fuels

Article

pubs.acs.org/EF

Synthesis and Evaluation of Terpolymers Consist of Methacrylates with Maleic Anhydride and Methacrylic Morpholine and Their Amine Compound as Pour Point Depressants in Diesel Fuels

Mingan Zhou, Yi He, Yanwei Chen, Yingpin Yang, Hualin Lin,* and Sheng Han*

School of Chemical and Environmental Engineering, Shanghai Institute of Technology, Shanghai 201418, People's Republic of China

Supporting Information

ABSTRACT: Long-chain alkyl (i.e., tetradecyl, hexadecyl, and octodecyl) methacrylate (MC), maleic anhydride (MA), and methylamidemorpholine ($MCNR_2$) were used in this study to prepare a series of MC−MA−$MCNR_2$ terpolymers and their amine compounds (MC−MA−$MCNR_2$−a) to obtain efficient pour point depressants (PPDs) for diesel fuel. The MC−MA−$MCNR_2$ and MC−MA−$MCNR_2$−a terpolymers were successfully synthesized and then characterized by Fourier transform infrared (FTIR) spectroscopy, proton nuclear magnetic resonance (^{1}H NMR), and gel permeation chromatography (GPC). The effects of the addition of the PPDs on the solid point (SP) and cold filter plugging point (CFPP) of diesel fuel were also investigated. Furthermore, the interactions between the additives and wax crystals were elucidated through differential scanning calorimetry (DSC), polarizing optical microscopy (POM), and rheological mechanics. Results indicate that all of the terpolymer PPDs significantly improved the performance of 0# diesel fuel samples at low temperature. PPDC2 displayed the best performance in decreasing the SP and CFPP of diesel fuel by 19 and 11 °C, respectively. In addition, DSC analysis showed that the terpolymer PPDs reduced the temperature of paraffin precipitation of diesel fuel. However, POM analysis showed that addition of the PPDs did not prevent wax precipitation completely but merely shifted the precipitation toward a lower temperature. Moreover, the addition of the terpolymer PPDs remarkably decreased the viscosity of diesel fuel.

1. INTRODUCTION

In cold areas or at low temperature, the cold flow properties of diesel fuel become poor because of precipitation of paraffin in the fuel. Paraffin can be effectively dispersed by a small amount of additive, which is referred to as pour point depressants (PPDs).[1−6] Such additives produce small, regularly shaped wax crystals through one or more postulated mechanisms, such as nucleation, adsorption, co-crystallization, and increase in wax solubility.[4]

A great many kinds of polymers have been developed and used as PPDs to influence the behavior of the paraffin crystal formation.[7−9] PPDs can be divided into non-comb type and comb type. The former includes ethylene−butene copolymers, ethylene−vinyl acetate copolymers,[10,11] and alkyl aromatics,[12] whereas the latter usually have long alkyl chains, including poly(alkyl methacrylates),[13] α-olefin copolymers,[14] and maleic anhydride (MA) polymers.[3,15−17] Recently, increasing attention has been paid to methacrylate (MC), MA, and methacrylamide ($MCNR_2$) copolymers (MC−MA−$MCNR_2$), which typically contain highly polar functional groups.[18,19] However, in-depth research on the mechanism and effect of the PPDs is necessary. High polarity may attain a surfactant characteristic, which is a basic prerequisite for dispersant potential. Polar nitrogen in polymers can function simultaneously as both wax dispersants and flow improvers in one component additive.

In the present study, we synthesized a series of terpolymers (MC−MA−$MCNR_2$) derived from long-chain alkyl (i.e., tetradecyl, hexadecyl, and octodecyl) MC, MA, and $MCNR_2$ and their amine compounds (MC−MA−$MCNR_2$−a) by free-radical polymerization. We also evaluated their influence on the flow properties of diesel fuel.

2. EXPERIMENTAL SECTION

2.1. Chemical Materials. Samples of 0# diesel fuel were provided by Sinopec Co., Ltd., Shanghai, China. The terpolymers (MC−MA−$MCNR_2$ and MC−MA−$MCNR_2$−a) were synthesized and purified in a laboratory. Moreover, other substances were purchased from Sinopharm Chemical Reagent Co., Ltd., China, and employed without further purification: 1-tetradecanol, hexadecanol, octadecanol, MC, MA, dichlorosulfoxide, triethylamine, morpholine, methylene chloride, hydroquinone, *p*-toluenesulfonic acid (PTSA), benzoyl peroxide, octadecylamine, and sodium carbonate anhydrous. All substances used were analytical-grade reagents.

2.2. Preparation of Monomers. Figure 1 shows the synthesis routine for the preparation of monomers and $MCNR_2$. The *n*-alkyl acrylates were prepared via the reaction of methyl MC and different *n*-alkyl alcohols (n = 14, 16, and 18) at a molar ratio of 1:1 under a nitrogen environment. Toluene is used as a solvent; PTSA is used as a catalyst; and hydroquinone is used as an inhibitor. Water was azeotropically separated using a Dean−Stark apparatus.[20] *n*-Alkyl alcohols, MC, toluene, PTSA, and hydroquinone were added to a three-necked flask and then gradually heated to 120 °C for approximately 5 h (when water is theoretically separated to a certain extent). The reaction products were washed for several times with an aqueous solution of Na_2CO_3 (5% m/V) until the underlayer of liquid was clarified. The products then washed with distilled water, and then these products were vacuum-distilled using a rotary evaporator and vacuum-dried. The end product obtained was either a light yellow or milky white latex substance.[21]

The most convenient method of obtaining methyl acryloyl chloride is through the reaction of methylacrylic acid and sulfoxide chloride.

Received: May 13, 2015
Revised: August 15, 2015

DOI: 10.1021/acs.energyfuels.5b01072
Energy Fuels XXXX, XXX, XXX−XXX

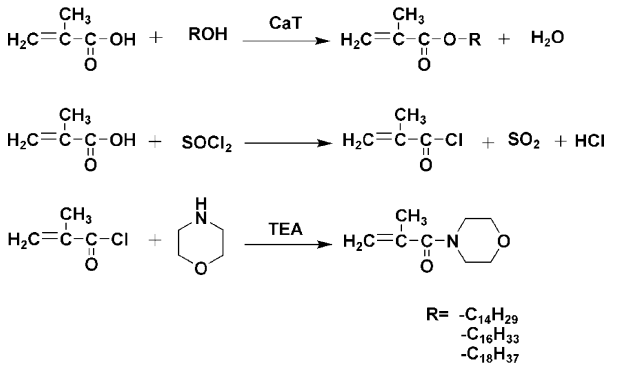

Figure 1. Synthetic routine for the preparation of monomers and $MCNR_2$.

Thus, sulfoxide chloride (1.1 equiv) was added dropwise at −10 °C to a stirred dichloromethane solution of methylacrylic acid (1 equiv). A small amount of hydroquinone (1%) acted as an inhibitor. After stirring for 30 min, the solution was slowly heated to 60 °C for approximately 6 h. Once the temperature reached 25 °C, the reaction system generated bubbles for escape. These bubbles were composed of a mixed gas containing sulfur dioxide and hydrogen chloride. Moreover, the fraction boiling range for the atmospheric distillation of methyl acryloyl chloride was 96−101 °C (yield is 75%).

Triethylamine (2 equiv) was added dropwise to a morpholine solution (1 equiv) in dry dichloromethane at 0 °C under a N_2 atmosphere, along with a corresponding dose of methyl acryloyl chloride (1.1 equiv). The resultant solution was left for over 6 h to warm to room temperature. Water was added and stirred after the reaction, and the layers were separated. The organic layer was washed with demineralized water, dried over sodium sulfate, and filtered. The solvent was removed under reduced pressure to yield a crude product, which was purified with column chromatography using a mixture of hexanes and ethyl acetate.[2,22]

2.3. Preparation of MC−MA−$MCNR_2$ and MC−MA−$MCNR_2$−a Terpolymers. The polymerization reaction is illustrated in Figure 2.

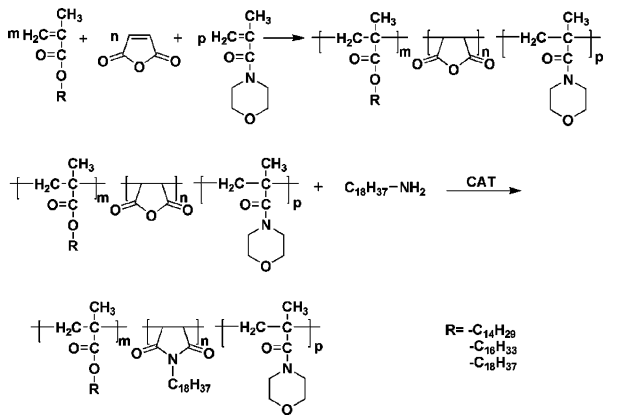

Figure 2. Synthetic routine for terpolymer preparation.

In a typical process, a three-neck round flask was fitted with a magnetic stirrer, a condenser, a temperature controller, and a nitrogen-controlled inlet valve. This flask was then filled stepwise with toluene solvent, long-chain alkyl (i.e., tetradecyl, hexadecyl, and octodecyl) MC, $MCNR_2$, and/or MA at a certain molar ratio. Nitrogen gas was flushed through the flask for 30 min, while the reaction mixture was gradually heated. The flushing process ceased when the temperature of the reactants reached 50 °C. The reaction mixture was then stirred vigorously for 6 h under a nitrogen blanket when the temperature increased to 100 °C. A solution of benzoyl peroxide toluene was added to the aforementioned reaction mixture as an initiator. When the reaction system had cooled to room temperature, excess methanol was added to the reaction solution. A white precipitate was obtained after filtration and then added to the toluene solvent. This procedure was repeated 3 times to remove impurities. After rotary evaporation, which was employed to remove toluene solvent, the terpolymers MC−MA−$MCNR_2$ were obtained and vacuum-dried for 24 h.[23] The resultant terpolymers were allowed to react with octodecylamine at a molar ratio of 1:1 for 8−10 h in the presence of molecular sieves at 140 °C. Toluene was used as a solvent. The terpolymers MC−MA−$MCNR_2$−a were obtained after the same purification process used for MC−MA−$MCNR_2$.

2.4. Composition of Fuels. The physicochemical characteristics are given in Table 1. Gas chromatography (GC, GC-2010, Shimadzu Corp.) was used to analyze the carbon number distribution of *n*-alkanes in the diesel fuel and their separation fractions (i.e., filtration and precipitate). The conditions of GC were as follows: the temperature of the capillary was increased from 120 to 280 °C at 5 °C/min; the interface temperature and injector temperature were 290 and 300 °C, respectively; and the diffluent ratio was 150:1. The compositions of the diesel by GC are given in Figure 3. The carbon number of the total wax is broadly distributed, and the average carbon number of *n*-paraffin is 14.5. The waxy diesel fuel includes 41.2 wt % *n*-paraffin, which generates strongly gelled networks. This result implies a very high wax content of diesel fuel, and thus, the cold flow properties of this duel fuel cannot be easily improved. The prepared PPDs that serve as wax crystal modifiers are particularly scheming substances with hydrophobic (long alkyl chains) and hydrophilic (polar morpholine groups) moieties. Therefore, we used a series of MC−MA−$MCNR_2$ and MC−MA−$MCNR_2$−a as ideally efficient crystal modifiers.

Table 1. Physical and Chemical Characteristics of Diesel Fuel

test	method	fuel
density at 20 °C (kg/m^3)	SH/T0604	841.4
kinematic viscosity at 40 °C (mm^2/s)	GB/T265	4.634
flash point (°C)	GB/T261	68
cold filter plugging point (°C)	SH/T0248	0
solid point (°C)	GB/T510	−8
S content (%, m/m)	SH/T0689	0.1533
saturated hydrocarbon (mass %)	MS	85.6
aromatic hydrocarbon (mass %)	MS	14.4
acidity (mg of KOH/100 mL)	GB/T258	2.10
16 alkyl index	GB/T388	51.9
boiling distillation (°C)	GB/T6536	282−377

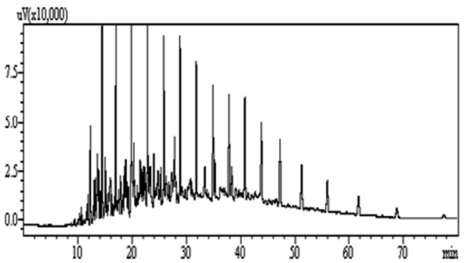

Figure 3. Concentration distribution of diesel measured by GC−MS.

2.5. Evaluation Tests of Cold Flow Performance. The tested diesel fuel samples were prepared individually by mixing the prepared terpolymers (MC−MA−$MCNR_2$ and MC−MA−$MCNR_2$−a) with diesel fuel in concentrations of 100, 200, 500, and 1000 ppm at 50 °C.[24] The samples were stirred for 40 min to dissolve the PPDs completely.[25] The cold flow performance, solid point (SP), and cold filter plugging point (CFPP) of the tested diesel samples were

DOI: 10.1021/acs.energyfuels.5b01072
Energy Fuels XXXX, XXX, XXX−XXX

measured according to ASTM D6371 and GB/T 510 standard methods.

2.6. Differential Scanning Calorimetry (DSC). DSC curves of the samples were recorded by a thermal analyzer (model Q2000 by TA Company) operating in the liquid-nitrogen subambient mode.[26] To investigate the interactions of polymeric additives with wax crystals in diesel fuel, thermal analysis via DSC was conducted to determine the wax appearance temperature (WAT) and enthalpy of the diesel sample. The instrument was calibrated using known transition temperatures and enthalpies of *n*-pentacosane and indium, which were obtained through DSC analysis during the cooling cycle at a scanning rate of 10 °C/min from +30 to −30 °C.[27]

2.7. Polarizing Optical Microscopy (POM). The POM analysis is a highly effective and intuitive way to study the influence of SP on the crystallization behavior of wax crystals.[28,29] We recorded photomicrographs that depicted the wax crystallization behavior of untreated 0# diesel fuel samples as well as those treated with PPDs. POM analysis was conducted with an Olympus polarizing microscope model BHSP, which was fitted with an automatic camera in a 35 mm format. A helium lamp was used as a light source. On the microscope slide, the temperature of the tested 0# diesel fuel sample was controlled using an attached cooling thermostat.

2.8. Viscosity. Viscosity is the most important rheological parameter because it not only affects the density of diesel fuel but also influences the flow properties.[30−34] Lower viscosity implies better low-temperature flow properties. The temperature is a significant factor that strongly influences the viscosity of diesel fuel. As the temperature decreases, the gel structures of the precipitated wax are formed gradually. Viscosity−temperature curves of the neat diesel fuel and diesel fuel with additives were obtained using an advanced rheometer (Anton Paar MCR302) equipped with coaxial cylinder geometry.

Prior to rheological measurement, the diesel fuel sample was conditioned at 50 °C for 30 min to reset the previous shear and thermal history of the diesel fuel.[35−37] The test temperature range is from +20 to −20 °C at a shear rate of 50 s^{-1}.

3. RESULTS AND DISCUSSION

3.1. Characterization of the Chemical Structures of Terpolymer PPDs. *3.1.1. Fourier Transform Infrared (FTIR) Spectroscopy.* The composition of the terpolymers was characterized with FTIR spectrometry in a Bio-Rad Excalibur Series FTS-3500GX system. The analysis method varied according to product characteristics. The alkyl MC monomers and terpolymers were analyzed as molten films between KBr cells. Figure 4 displays the FTIR spectra of MC−MA−$MCNR_2$ and MC−MA−$MCNR_2$−a and clearly illustrates all of the characteristic CH_3 and CH_2 absorption peaks of long- or short-chain alkyls at 2921 and 2852 cm^{-1}. This figure also presents the strong characteristic C═O absorption peak of tetradecyl MC at 1732 cm^{-1} and the two characteristic C═O stretching peaks of MA at 1857 and 1783 cm^{-1}. The characteristic C═C stretching vibration peak of tetradecyl MC vanishes completely. The typical swing absorption peaks of characteristic −CH_2− in long-chain alkyl are detected at 721 cm^{-1}. In particular, spectra b and d of Figure 4 indicate that the amidation reaction is generated as expected, that the characteristic C−N stretching peak is detected at 1406 cm^{-1}, and that the characteristic of the amide group is evident. These findings suggest that chain alkyl MA and $MCNR_2$ are present in the prepared terpolymers.

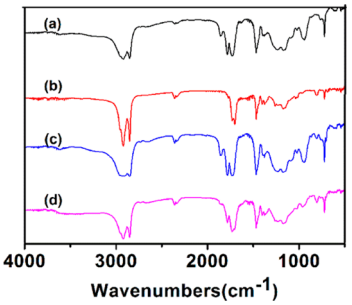

Figure 4. FTIR spectra of (a) 14MC, (b) $MCNR_2$, (c) 14MC−MA−$MCNR_2$, and (d) 14MC−MA−$MCNR_2$−a.

3.1.2. Proton Nuclear Magnetic Resonance (^{1}H NMR). The chemical structures of the prepared MC−MA−$MCNR_2$ and MC−MA−$MCNR_2$−a terpolymers were characterized further through ^{1}H NMR analysis. Figure 5 exhibits the typical ^{1}H NMR spectra of the terpolymers. However, the peaks of H of the polymeric state MA and the polymeric state morpholine are not obvious. H of the methylene group adjacent to the oxygen atom of tetradecyl is generated at a chemical shift of 3.970 ppm. H of the methylene adjacent to methylene, which is, in turn, adjacent to the oxygen atom of tetradecyl, is observed at a chemical shift of 1.601 ppm. Moreover, H in the long-chain methylene bands is detected at shifts ranging from 1.302 to 1.263 ppm, and the methyl group exhibits a chemical shift at 0.897−0.863 ppm. Panels a and b of Figure 5 differ only in terms of the peak area of long-chain methylene bands. These results also indicate that the prepared terpolymers contain chain alkyl, MC, and methacrylicmorpholine moieties.

3.1.3. Gel Permeation Chromatography (GPC). The molecular weights and polydispersity index of the terpolymers were determined using GPC. The mobile phase was $CHCl_3$, with a flow rate of 1 mL/min. Polystyrene was used as the standard substance, and the results are presented in Table 2. In general, a molecular weight between 4000 and 100 000 g/mol PPD effectively limits SP and CFPP. The molecular weights of the all of the terpolymers remained within the preferred molecular weight range, and the differences between them were insignificant. Furthermore, the polydispersity index value ranges from 2.002 to 3.651. The GPC results indicated that the degrees of polymerization of the terpolymers are very suitable, and they are highly applicable as PPDs of diesel fuel.

Through FTIR, ^{1}H NMR, and GPC tests, we found that the synthesized terpolymers was random terpolymers.

3.2. SP and CFPP. *3.2.1. Effect of MC−MA−$MCNR_2$.* The effects of the synthesized MC−MA−$MCNR_2$ on the SP and CFPP depressions of diesel fuel are summarized in Table 3. Each polymeric additive effectively reduced SP, and this effectiveness increased with the increase in the concentration of additive in the diesel. SP and CFPP were decreased with the increase in the amount of additive. In particular, a 500 ppm dose is effective. However, doses exceeding 500 ppm may depress SP further, and thus, excessive doses of additive are not economically advisible.[38]

14MC−MA−$MCNR_2$ (MC/MA = 1:1) reduces SP (by 18 °C) and CFPP (by 6 °C) most significantly at a concentration of 500 ppm. At the same concentration, 14MC−MA−$MCNR_2$ (MC/MA = 1:2) lowers SP and CFPP by 15 and 4 °C, respectively. Although 16MC−MA−$MCNR_2$ and 18MC−MA−$MCNR_2$ were similar to 14MC−MA−$MCNR_2$, they were ineffective with respect to SP and CFPP reduction. This finding may be attributed to the fact that the *n*-alkyl chain lengths of PPDs significantly affect the reduction extent of SP and CFPP. Thus, this effect is expected because the influence of the *n*-alkyl chain lengths of terpolymers is closely related to the content of the corresponding *n*-alkane in the diesel fuel, especially the effect on SP. The long hydrocarbon paraffin

DOI: 10.1021/acs.energyfuels.5b01072
Energy Fuels XXXX, XXX, XXX−XXX

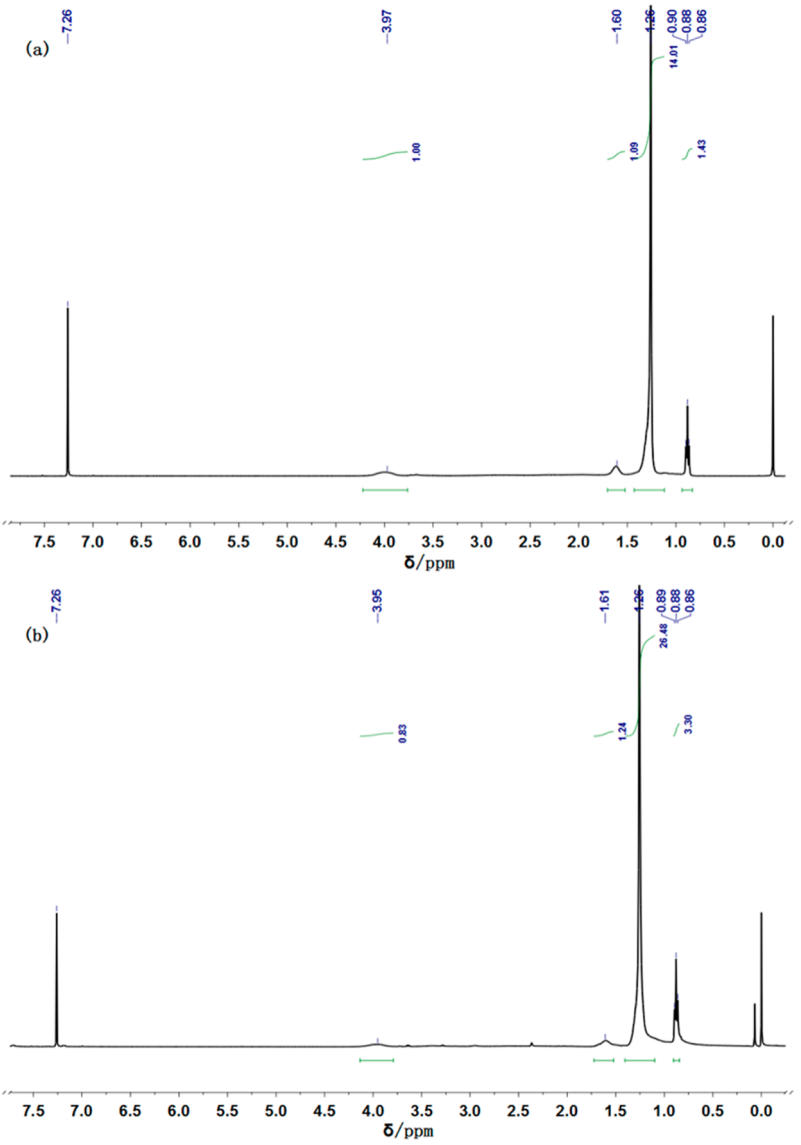

Figure 5. ^{1}H NMR spectra of (a) 14MC−MA−MCNR$_2$ and (b) 14MC−MA−MCNR$_2$−a.

Table 2. Molar Mass of Terpolymers[a]

terpolymer	MC/MA	M_w (g/mol)	M_n (g/mol)	M_w/M_n
14MC−MA−MCNR$_2$	1:1	15420	6693	2.304
14MC−MA−MCNR$_2$−a	1:1	20548	7538	2.714
14MC−MA−MCNR$_2$	1:2	13090	6090	2.149
14MC−MA−MCNR$_2$−a	1:2	26356	7216	3.651
16MC−MA−MCNR$_2$	1:1	19774	9874	2.002
16MC−MA−MCNR$_2$−a	1:1	20169	10038	2.009
16MC−MA−MCNR$_2$	1:2	17410	7538	2.309
16MC−MA−MCNR$_2$−a	1:2	16543	7359	2.248
18MC−MA−MCNR$_2$	1:1	17822	8894	2.004
18MC−MA−MCNR$_2$−a	1:1	25272	11308	2.235
18MC−MA−MCNR$_2$	1:2	19670	7330	2.683
18MC−MA−MCNR$_2$−a	1:2	19818	9339	2.122

[a]All terpolymer proportions of MC/MCNR$_2$ = 1:1.

chains tend to interact with the polymer alkyl groups, which act as crystallization nuclei that hang from the polymeric matrix. Therefore, numerous crystallization nuclei correspond to fewer free paraffin molecules. Fluidity is hindered at a low temperature, thereby decreasing the SP. However, a high quantity of long-chain groups can disrupt the crystallization on the polymer chain through steric hindrance.[5] Meanwhile, when the content of MA was increased, the effect did not change considerably.

3.2.2. Effect of MC−MA−MCNR$_2$−a. The effects of the synthesized MC−MA−MCNR$_2$−a on the SP and CFPP depressions of diesel fuel are summarized in Table 4. All MC−MA−MCNR$_2$−a are less effective with regard to SP and CFPP reduction than the MC−MA−MCNR$_2$. This difference is probably because the C−O bond (high polarity) was replaced by the C−N bond (low polarity) when primary amine aminating anhydride was used. Thus, the decrease in the effect of coagulation is due to the decreased polarity of PPD. This polarity may reach a surfactant character, which is considered the basic prerequisite for dispersants.

Nonetheless, these PPDs positively affected SP and CFPP when mixed up, as presented in Table 5. This phenomenon is ascribed to the fact that the morphology of these combined PPDs was similar to that of the wax crystals in the diesel fuel.

DOI: 10.1021/acs.energyfuels.5b01072
Energy Fuels XXXX, XXX, XXX−XXX

Table 3. ΔSP (°C) and ΔCFPP (°C) of Diesel Fuel Treated with MC−MA−MCNR$_2$

terpolymer	additive concentration (ppm)	MC/MA	ΔSP (°C)	ΔCFPP (°C)
14MC−MA−MCNR$_2$	100	1:1	10	2
	100	1:2	14	3
	200	1:1	12	3
	200	1:2	14	3
	500	1:1	18	6
	500	1:2	15	4
	1000	1:1	14	4
	1000	1:2	13	3
16MC−MA−MCNR$_2$	100	1:1	6	2
	100	1:2	6	1
	200	1:1	7	2
	200	1:2	6	1
	500	1:1	9	2
	500	1:2	9	2
	1000	1:1	7	2
	1000	1:2	6	2
18MC−MA−MCNR$_2$	100	1:1	7	1
	100	1:2	6	2
	200	1:1	7	1
	200	1:2	6	2
	500	1:1	9	3
	500	1:2	9	3
	1000	1:1	6	1
	1000	1:2	6	3

Table 4. ΔSP (°C) and ΔCFPP (°C) of Diesel Fuel Treated with MC−MA−MCNR$_2$−a

terpolymer	additive concentration (ppm)	MC/MA	ΔSP (°C)	ΔCFPP (°C)
14MC−MA−MCNR$_2$−a	100	1:1	6	1
	100	1:2	6	4
	200	1:1	6	2
	200	1:2	6	4
	500	1:1	10	4
	500	1:2	8	5
	1000	1:1	5	3
	1000	1:2	8	5
16MC−MA−MCNR$_2$−a	100	1:1	5	1
	100	1:2	4	1
	200	1:1	7	1
	200	1:2	4	1
	500	1:1	8	2
	500	1:2	8	2
	1000	1:1	4	2
	1000	1:2	4	2
18MC−MA−MCNR$_2$−a	100	1:1	6	2
	100	1:2	7	3
	200	1:1	5	2
	200	1:2	7	3
	500	1:1	7	3
	500	1:2	7	3
	1000	1:1	6	2
	1000	1:2	7	2

3.3. DSC Analysis. DSC can be used for quantitative analysis of energy changes in the phase change process of diesel fuel[39] at a low temperature. Figure 6 depicts the thermograms of the diesel fuels with and without terpolymer PPDs. The DSC curves of wax all shifted to a lower temperature after the PPDs were added to the paraffin mixtures. In addition, a remarkable difference is found in the WAT of neat and PPD-treated diesel fuel; the WAT of diesel fuel is 4.5 °C, whereas the WATs of PPD-treated diesel fuels have shifted to a lower temperature. Table 5 shows the phase transition temperatures and energies obtained from the prominent peaks of the thermograms.

The starting temperature of the peak (onset) at the curves reflects that of wax crystal precipitation in diesel. The slope of the peak denotes the rate of precipitation, and solid−liquid phase change energy (ΔH) corresponds to dispersion stability.[40,41] Table 6 also depicts the starting temperature (onset), peak temperature (peak), and absolute value of the ΔH of diesel fuel as well as those PPD-treated diesel fuels. The starting temperature (onset) of 0# diesel fuel is 3.1 °C, and the absolute value of the ΔH of diesel fuel is 1.830 J/g. All of the onset and ΔH values of the PPDs were lower than the values of diesel fuel. In particular, PPDC2 is considerably reduced when its onset temperature is −3.06 °C and its ΔH value is 1.136 J/g. These results indicate that PPDs act as paraffin dispersants in diesel fuel, thereby delaying the paraffin crystallization

Table 5. ΔSP (°C) and ΔCFPP (°C) of Diesel Fuel Treated with Combined Terpolymer Additives

	composition in the terpolymers (mol %)						
	MC−MA−MCNR$_2$		MC−MA−MCNR$_2$−a				
sample	14	18	14	18	additive concentration (ppm)[a]	ΔSP (°C)	ΔCFPP (°C)
PPDC1	50	50			500	16	5
PPDC2	50			50	500	26	11
PPDC3			50	50	500	15	5
PPDC4		50	50		500	23	9

[a]The additive concentration of each single PPD is 500 ppm.

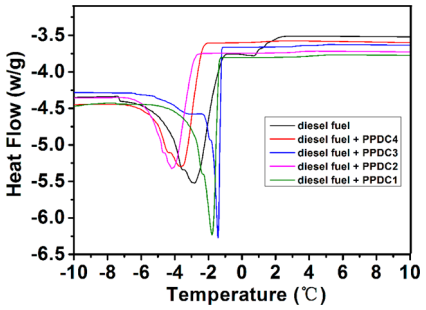

Figure 6. DSC thermograms of diesel fuel and diesel fuel with PPDs in a 500 ppm concentration.

Table 6. Data Analysis of DSC

sample	onset (°C)	peak (°C)	endset (°C)	ΔH (J/g)	peak area (mJ)
diesel fuel	3.1	−2.81	−7.58	1.830	449.56
diesel fuel + PPDC1	−1.25	−1.42	−5.23	1.219	329.24
diesel fuel + PPDC2	−3.06	−4.18	−7.84	1.136	207.76
diesel fuel + PPDC3	−1.17	−1.48	−6.27	1.490	361.59
diesel fuel + PPDC4	−2.49	−3.49	−7.12	1.140	257.12

DOI: 10.1021/acs.energyfuels.5b01072
Energy Fuels XXXX, XXX, XXX−XXX

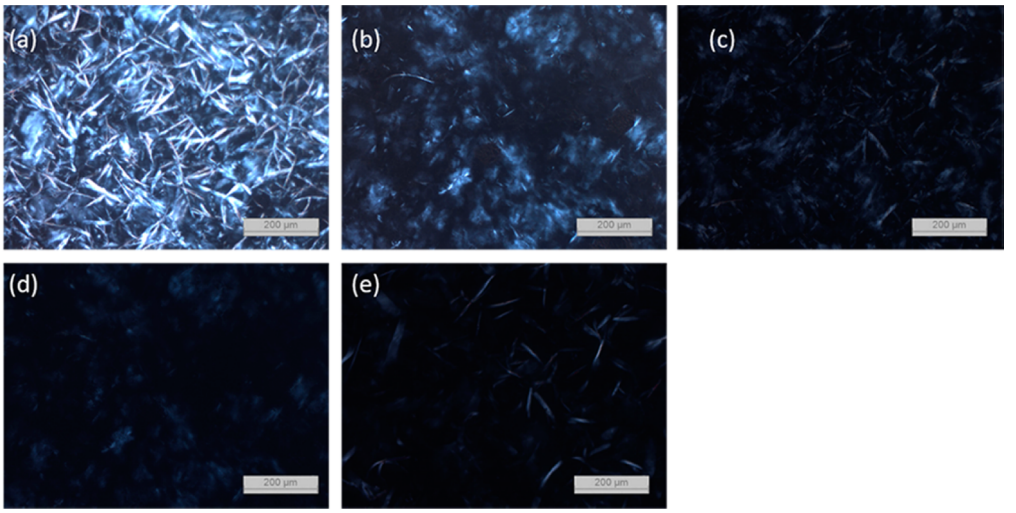

Figure 7. POM images of crystal morphologies of (a) diesel fuel at −10 °C, (b) diesel fuel with PPDC1 at −10 °C, (c) diesel fuel with PPDC2 at −10 °C, (d) diesel fuel with PPDC3 at −10 °C, and (e) diesel fuel with PPDC4 at −10 °C.

temperature. This finding is in accordance with the changes in SP and CFPP of diesel fuel (Table 4). Moreover, all of the PPD ingredients are present in nitrogen heterocyclic groups (morpholine). Thus, these terpolymers have strong polarity and high steric hindrance. Terpolymers themselves cannot solidify easily to become nuclei. As a result, the phase change temperature is lowered when PPDs are added to 0# diesel fuel.

3.4. POM Analysis. The influence of additives on the size, shape, and aggregation of wax crystals was studied through POM. Figure 7 displays the microscopic images of diesel fuel wax crystals with or without PPDs. Figure 7a indicates that the wax crystals formed from diesel fuel at −10 °C, whereas panels b−e of Figure 7 illustrate the wax crystals generated when terpolymer additives were added to 0# diesel fuel at −10 °C.

The wax crystals that formed in the diesel fuel in the system are lenient and tableted, thus indicating their growth at nucleating sites. However, the shapes of these wax crystals changed to a frazil crystal state in the presence of PPDs. Figure 7c suggests the existence of the least amount and smallest fine needles. Thus, PPDC2 show the optimal fluidity. This observation agrees with the findings from the SP/CFPP and DSC experiments in this study. On the basis of the photomicrographs, two molecular forces collaborate to generate aggregates during wax accumulation. First, the polar groups (morpholine) of the PPDs can interact with one another or with paraffin through a $\pi-\pi$ stacking attractive force, which serves as a dispersant. Second, the existence of the long-chain alkyl can match the carbon number of paraffin, which hinders paraffin aggregation. Therefore, these PPDs effectively delayed the aggregation of crystals at a low temperature and modified the crystallization behavior of these crystals by transforming their shape and depressing the formation of large crystals.

3.5. Viscosity Analysis. The variations in viscosity of neat diesel fuel and diesel fuel with PPDs at different temperatures are given in Figure 8. The viscosity of both untreated and treated fuel at temperatures higher than a temperature point (which is very near their CFPP) is very low because of the low paraffin content in diesel fuel. However, when the temperature continues to decrease, the viscosity of diesel fuel rapid increases, even higher than the treated fuel; among them, diesel fuel treated with PPDC2 exhibits the best performance. This behavior may be explained by the two reasons: On the one

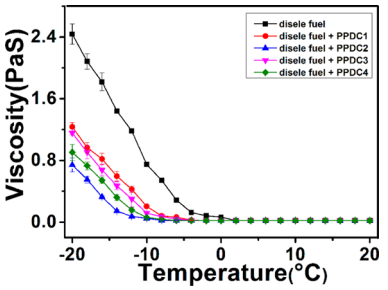

Figure 8. Viscosity−temperature curves of diesel fuel and with PPDs in a 500 ppm concentration.

hand, PPDs have changed the morphology of paraffin molecules in diesel fuel, resulting in a decrease in CFPP, thereby reducing the temperature at which viscosity increases. On the other hand, the intermolecular forces of paraffin in diesel fuel become weaker when PPDs are added because of nucleation, by which the paraffin molecules are dispersed. As a result, viscosity is reduced.

4. CONCLUSION

(1) A series of terpolymers derived from alkyl MC, MA, and $MCNR_2$ was prepared, purified, and characterized. These polymers possess differently structured polar functional groups. (2) Experimental results showed that all polymeric additives were efficient as PPDs and flow improvers in diesel fuel. The prepared PPDC2 performs a dual function, i.e., as both a wax dispersant and a flow improver. Moreover, all of the additives effectively decreased SP and CFPP. In particular, their CFPP depression performance is optimal. (3) DSC analysis showed that these terpolymers act as a paraffin dispersant in diesel fuel, in which they lowered the temperature at which paraffin wax is formed (i.e., WAT). In the process, cold flow fluidity is significantly transformed. (4) POM analysis showed that the terpolymers do not completely prevent paraffin precipitation; they merely shift the precipitation toward a lower temperature. (5) All of the PPDs reduced the viscosity of diesel fuel and improved its low-temperature flowability by changing the intermolecular force of paraffin molecules in diesel fuel. (6) The higher pour point depression activity of the terpolymer may be attributed to the combined effects of carbonyl oxygen of

DOI: 10.1021/acs.energyfuels.5b01072
Energy Fuels XXXX, XXX, XXX−XXX

maleic anhydride and the polarity exerted by the cycloether linkage of amide polar functional groups (morpholine group) of the terpolymer structure. Thus, these results indicate that the terpolymers with carbonyl oxygen of maleic anhydride and amide polar functional groups (MC−MA−$MCNR_2$ and MC−MA−$MCNR_2$−a) possess good pour point depression activity, and the PPDs are the excellent cold flow improvers to 0# diesel fuel.

■ ASSOCIATED CONTENT

Supporting Information

The Supporting Information is available free of charge on the ACS Publications website at DOI: 10.1021/acs.energyfuels.5b01072.

All ^{1}H NMR spectra of methyl methacrylate, methyl acryloyl morpholine, MC−MA−$MCNR_2$, and MC−MA−$MCNR_2$−a and all FTIR spectra of methyl acrylamide morpholine, MC−MA−$MCNR_2$, and MC−MA−$MCNR_2$−a (PDF)

■ AUTHOR INFORMATION

Corresponding Authors

*Telephone: +86-021-6087-3560. E-mail: lhl65343@163.com.
*Telephone: +86-18917950352. E-mail: hansheng654321@sina.com.

Notes

The authors declare no competing financial interest.

■ ACKNOWLEDGMENTS

This project was supported by the Shanghai Leading Academic Discipline Project (Project J51503), the National Natural Science Foundation of China (Project 20976105), the Science and Technology Commission of Shanghai Municipality (Project 09QT1400600), the ShuGuang Project (Project 11SG54), the Innovation Program of Shanghai Municipal Education Commission (Project 11ZZ179), the Innovation Program of Shanghai Municipal Education Commission (Project 09YZ387), the Shanghai Talent Development Funding (Project 201335), and the Pujiang Talent Project (13PJ1407400) from the Science and Technology Commission of Shanghai Municipality.

■ REFERENCES

(1) An, H.; Gao, S. G.; Li, S.; Xie, Y. X. *Adv. Mater. Res.* **2011**, *236*−*238*, 708−714.
(2) Shi, F.; Smith, M. R.; Maleczka, R. E. *Org. Lett.* **2006**, *8* (7), 1411−1414.
(3) Zhang, H.; Liu, H.; Wang, S. *Pet. Sci.* **2009**, *6* (1), 82−85.
(4) Botros, M. G. U.S. Patent 5,681,359, 1997.
(5) Han, S.; Song, Y. P.; Ren, T. H. *Energy Fuels* **2009**, *23* (5), 2576−2580.
(6) Ghosh, P.; Das, M. *J. Pet. Sci. Eng.* **2014**, *119*, 79−84.
(7) Cao, K.; Zhu, Q. J.; Wei, X. X.; Yao, Z. *Energy Fuels* **2015**, *29*, 993−1000.
(8) Lu, Y.; Zhang, X.; Yao, G. C. *Energy Fuels* **2011**, *25*, 2115−2118.
(9) Liu, T.; Fang, L.; Liu, X.; Zhang, X. D. *Fuel* **2015**, *143*, 448−454.
(10) Ashbaugh, H. S.; Guo, X.; Schwahn, D.; Prud'homme, R. K.; Richter, D.; Fetters, L. J. *Energy Fuels* **2005**, *19* (1), 138−144.
(11) Taraneh, J. B.; Rahmatollah, G.; Hassan, A.; Alireza, D. *Fuel Process. Technol.* **2008**, *89* (10), 973−977.
(12) Kuzmic, A. E.; Radosevic, M.; Bogdanic, G.; Vukovic, R. *Fuel* **2007**, *86*, 1409−1416.
(13) Du, T.; Wang, S. J.; Song, C. P.; Liu, H. Y.; Nie, Y. D. *Acta Pet. Sin., Pet. Process. Sect.* **2010**, *26*, 812−818 (in Chinese)..
(14) Zhang, Y. H.; Zhuo, R. S.; Ye, T. X.; Sun, Y. *Acta Pet. Sin., Pet. Process. Sect.* **2005**, *21*, 83−87 (in Chinese)..
(15) Deshmukh, S.; Bharambe, D. P. *Fuel Process. Technol.* **2008**, *89* (3), 227−233.
(16) Xu, J.; Qian, H.; Xing, S.; Li, L.; Guo, X. *Energy Fuels* **2011**, *25* (2), 573−579.
(17) El-Ghazawy, R. A.; Farag, R. K. *J. Appl. Polym. Sci.* **2010**, *115* (1), 72−78.
(18) Wu, Y.; Ni, G.; Yang, F.; Li, C.; Dong, G. *Energy Fuels* **2012**, *26* (2), 995−1001.
(19) (a) Fang, L.; Zhang, X. D.; Ma, J. H.; Zhang, B. T. *Ind. Eng. Chem. Res.* **2012**, *51*, 11605−11612. (b) Ghosh, P.; Das, M. *J. Pet. Sci. Eng.* **2014**, *119*, 79−84.
(20) Soni, H. P.; Bharambe, D. P. *Iran. Polym. J.* **2006**, *15* (12), 943−954.
(21) Feng, L.; Zhang, Z.; Wang, F.; Wang, T.; Yang, S. *Fuel Process. Technol.* **2014**, *118*, 42−48.
(22) Raghunathan, R.; Kumarasamy, E.; Iyer, A.; Ugrinov, A.; Sivaguru, J. *Chem. Commun.* **2013**, *49* (77), 8713−8715.
(23) Deshmukh, S.; Bharambe, D. *Fuel Process. Technol.* **2008**, *89* (3), 227−233.
(24) Castro, L. V.; Flores, E. A.; Vazquez, F. *Energy Fuels* **2011**, *25* (2), 539−544.
(25) Soni, H. P.; Kiranbala; Agrawal, K.; Nagar, A.; Bharambe, D. P. *Fuel Process. Technol.* **2010**, *91* (9), 997−1004.
(26) Castro, L. V.; Vazquez, F. *Energy Fuels* **2008**, *22* (6), 4006−4011.
(27) Bicerano, J. *Prediction of Polymer Properties*; CRC Press: Boca Raton, FL, 2002.
(28) Al-Sabagh, A.; Sabaa, M.; Saad, G.; Khidr, T.; Khalil, T. *Egypt. J. Pet.* **2012**, *21* (1), 19−30.
(29) Yi, S.; Zhang, J. *Energy Fuels* **2011**, *25* (12), 5660−5671.
(30) Santos, N.; Rosenhaim, R.; Dantas, M.; Bicudo, T.; Cavalcanti, E.; Barro, A.; et al. *J. Therm. Anal. Calorim.* **2011**, *106*, 501−506.
(31) Joshi, R.; Pegg, M. *Fuel* **2007**, *86*, 143−151.
(32) Conceição, M. M.; Candeia, R. A.; Dantas, H. J.; Soledade, L. E. B.; Fernandes, V. J.; Souza, A. G. *Energy Fuels* **2005**, *19* (5), 2185−2188.
(33) Alicke, A. A.; Leopércio, B. C.; Marchesini, F. H.; de Souza Mendes, P. R. *Fuel* **2015**, *140*, 446−452.
(34) Chen, B. S.; Sun, Y. Q.; Fang, J. H.; Wang, J.; Wu, J. *Biomass Bioenergy* **2010**, *34* (9), 1309−1313.
(35) Singh, P.; Fogler, H. S.; Nagarajan, N. R. *J. Rheol.* **1999**, *43*, 1437−1459.
(36) Ashbaugh, H. S.; Fetters, L. J.; Adamson, D. H.; Prud'homme, R. K. *J. Rheol.* **2002**, *46*, 763−776.
(37) Petter Rønningsen, H. *J. Pet. Sci. Eng.* **1992**, *7*, 177−213.
(38) Deshmukh, S.; Bharambe, D. *Energy Sources, Part A* **2012**, *34* (12), 1121−1129.
(39) Quinchia, L. A.; Delgado, M. A.; Valencia, C.; Franco, J. M.; Gallegos, C. *J. Agric. Food Chem.* **2011**, *59* (24), 12917−12924.
(40) Srivastava, S.; Tandon, R.; Verma, P.; Pandey, D.; Goyal, S. *Fuel* **1995**, *74* (6), 928−931.
(41) Chatterjee, A. K.; Phatak, S. D.; Murthy, P. S.; Joshi, G. C. *J. Appl. Polym. Sci.* **1994**, *52* (7), 887.

DOI: 10.1021/acs.energyfuels.5b01072
Energy Fuels XXXX, XXX, XXX−XXX